The Astrophysical Journal, 706:L197–L202, 2009 November 20 doi:10.1088/0004-637X/706/1/L197

RUBBLE-PILE RESHAPING REPRODUCES OVERALL ASTEROID SHAPES

P. Tanga[1], C. Comito[1,7], P. Paolicchi[2], D. Hestroffer[3], A. Cellino[4,8], A. Dell'Oro[4], D. C. Richardson[5], K. J. Walsh[6], and M. Delbo[6]

[1] UMR 6202 Cassiopée, University of Nice-Sophia Antipolis, CNRS, Observatoire de la Côte d'Azur, BP 4229, 06304 Nice Cedex 4, France
[2] Dipartimento di Fisica, Università di Pisa, Largo Pontecorvo 3, 56127 Pisa, Italy
[3] Institut de Mécanique Céleste et de Calcul des Éphémérides (IMCCE), CNRS, Observatoire de Paris, 75014 Paris, France
[4] INAF/Osservatorio Astronomico di Torino, Via Osservatorio 20, 10122 Pino Torinese, Italy
[5] Department of Astronomy, University of Maryland, College Park, MD 20742-2421, USA
[6] UMR 6202 Cassiopée, University of Nice-Sophia Antipolis, CNRS, Observatoire de la Côte d'Azur, BP 4229, 06304 Nice Cedex 4, France
Received 2009 June 12; accepted 2009 October 22; published 2009 November 6

ABSTRACT

There have been attempts in the past to fit the observed bulk shapes (axial ratios) of asteroids to theoretical equilibrium figures for fluids, but these attempts have not been successful in many cases, evidently because asteroids are not fluid bodies. So far, however, the observed distribution of asteroid macroscopic shapes has never been attributed to a common cause. Here, we show that a general mechanism exists, capable of producing the observed shape distribution. We base our approach on the idea that aggregates of coherent blocks held together mostly by gravity (gravitational aggregates) can change their shape under the action of external factors, such as minor collisions, that break the interlocking of the constituent blocks, thus allowing them to asymptotically evolve toward fluid equilibrium. We show by numerical simulations that this behavior can produce a shape distribution compatible with the observations. Our results are shown to be consistent with a simple interpretation based on the topology of the potential energy field for rotating bodies. Also, they suggest that most asteroids have an internal structure that is at least partially fragmented, consistent with constraints derived from large asteroids (diameters >100 km) with satellites.

Key words: methods: *N*-body simulations – minor planets, asteroids – planets and satellites: formation – gravitation

1. INTRODUCTION

The theory of self-gravitating bodies at fluid equilibrium (Chandrasekhar 1969) predicts the existence of stable and continuous shape sequences for oblate spheroids (Maclaurin sequence) and triaxial ellipsoids (Jacobi sequence). Even though theoretical equilibrium figures remain a useful reference to approximate the most stable configurations (Farinella et al. 1981), in principle they cannot be applied to non-fluid bodies such as the asteroids. This is confirmed by an analysis of the distribution of asteroid shapes (approximated as ellipsoids; Figure 1) in the publicly available data set derived from photometric-based determinations of asteroid poles and overall shapes maintained at the Poznan observatory (Kryszczynska et al. 2007). It is evident that the distribution of observed shapes does not follow the theoretical trend corresponding to the equilibrium sequences for fluids.

However, according to numerical simulations of the overall process of collisional evolution (Michel et al. 2001; Davis et al. 2002), a significant fraction of the observed asteroids is expected to consist of fragmented bodies held together by gravity only ("rubble piles," or cohesionless gravitational aggregates). The typical size of the largest fragments may be around a few hundred meters.

Hard contacts among constituent blocks of different sizes may prevent the overall shape of a rubble-pile asteroid to come to fluid equilibrium. Estimates of shape and density have been used to compare asteroid properties with models that parameterize the effects of internal friction in terms of a "friction angle" or "angle of repose," namely, the maximum slope that a granular material can sustain, in the frame of the Mohr–Coulomb models (Holsapple 2001, 2004).

It is unknown whether large bodies (∼100 km or larger in diameter) are likely to be rubble piles, since this may depend on increasingly rare shattering/reaccumulating impacts for such large bodies over the age of the solar system. Nevertheless, bodies in the 100 km diameter size range could still change their shape due to heavy cratering, bulk motion of thick debris covering their cores, or overall material plasticity at these self-gravitating pressures.

In principle, any object (represented for the sake of simplicity as a triaxial ellipsoid) can be characterized by four parameters: the semi-axis ratios b/a and c/a (where $a \geqslant b \geqslant c$ are the semi-axis lengths), the normalized spin

$$\langle\omega\rangle = \omega/(\pi G\rho)^{1/2} \tag{1}$$

and the normalized angular momentum

$$\langle L\rangle = L/(Gm^3R)^{1/2}, \tag{2}$$

where m is the mass of the asteroid, R is its average radius, and ρ is its bulk density.

Under certain conditions (hydrostatic equilibrium, uniform rotation, and homogeneity), the above parameters are mutually dependent, and produce the sequences of equilibrium shapes of Chandrasekhar.

The comparison of theoretical shapes and observations is usually conducted in the $(c/a, \langle\omega\rangle^2)$ plane. Observed departures from the theoretical equilibrium sequence can be interpreted in terms of an estimated friction angle of ∼30° for asteroids (Holsapple 2001; Sharma et al. 2009). This value seems to be well justified, being close to the one exhibited by rock piles on the Earth.

[7] Also at: INAF Osservatorio Astronomico di Torino, Pino Torinese, Torino, Italy.
[8] Chercheur invité at IMCCE, Observatoire de Paris, France.

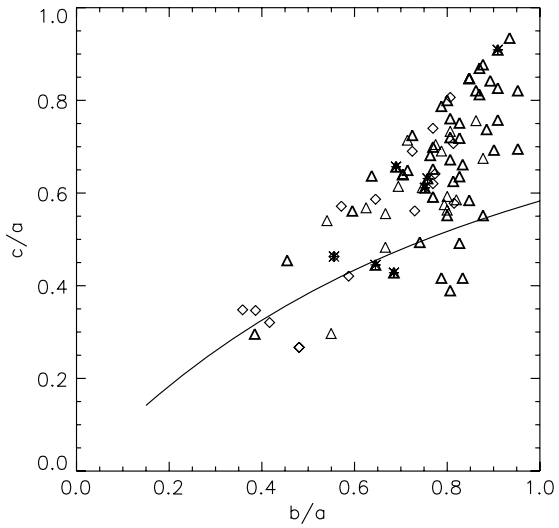

Figure 1. Distribution of known asteroid shapes, approximated by triaxial ellipsoids (Kryszczynska et al. 2007). Only objects for which both axis ratios have been determined are plotted. This data set is different from the one used for comparison to the Mohr–Coulomb theory in Holsapple (2001, 2004), in which only light-curve amplitude is used to infer b/a. Photometric inversion to obtain more complex shapes is possible (Kaasalainen et al. 2002, 2004), but the results can generally be well approximated by ellipsoids (Torppa et al. 2008) and the distribution remains similar. Objects marked by asterisks in the plot are large primary bodies (diameters $D > 100$ km) of high-size-ratio binary systems. Other symbols are used to distinguish bodies with $D < 50$ km (diamonds), 50 km $< D < 100$ km (thin triangles), and $D > 100$ km (bold triangles). The curved line in the plot represents the Jacobi sequence. The Maclaurin sequence coincides with the $b/a = 1$ line.

A limit in this kind of studies is due to the fact that, while the spin period is easily obtained from photometric variations, the normalization factor in Equation (1) requires estimating the bulk density of the object. Due to the usually large uncertainties associated to both size and mass determinations (Hilton 2002) (or to lack of data), best-guess values for these parameters, based on plausible mineralogy considerations, have to be assumed. Also, the polar flattening c/a is not accurately determined for most objects, introducing further uncertainties (Harris et al. 2009).

In this Letter, we try to explain what we know about asteroid shapes following an approach based on the assumption that any fragmented structure could progressively reshape via gradual rearrangement of the constituent blocks when subject to the action of gravity tides, non-disruptive impacts, seismic shaking, etc. Radiative spin-up (the YORP effect) is also capable of inducing a very efficient reshaping process in small asteroids (Walsh et al. 2008; Harris et al. 2009) (diameters < 10 km). We note that, interestingly, YORP should be able to produce also in several cases a spin-down effect, partly explaining the existence of slow rotators among small asteroids (Kitazato et al. 2007; Vokrouhlicky et al. 2007). For larger objects, which are insensitive to YORP, numerical simulations (Korycansky & Asphaug 2003; Richardson et al. 2005) indicate that asteroids may move closer to fluid equilibrium while reshaping after a collisional event.

An analogy can be found with granular piles, even those with intrinsically high angles of friction, that can be induced to flatten, by shaking mechanisms (Sánchez & Scheeres 2009). In other words, granular material, under certain conditions, can be induced to behave as if it had a low angle of friction, approaching fluid equilibrium.

Instead of simulating the external factors that induce reshaping, we decided to focus on the behavior of material with a very low friction angle (5°–10°), by simply assuming that those factors are operating, simulating the evolution of the structures, and checking afterward if our simulated end states could be compatible with the observed asteroid properties.

In particular, we create ellipsoidal rubble piles of arbitrary (b/a, c/a, $\langle\omega\rangle$ $\langle L\rangle$) combination, not corresponding to fluid equilibrium, and we follow their reshaping in isolation as they attempt to reach a more stable configuration. Details are provided in Section 2. For measuring the "distance" between an arbitrary ellipsoidal object and theoretical fluid equilibrium, we also revisited the classical computations of energy potential for self-gravitating fluids (Section 3).

We will show that the energy potential for fluid shapes plays a primary role, strongly influencing the reshaping process. Our final outcomes are compatible with the observed shape distribution on asteroids. Implications and result validation against several numerical issues are discussed in Section 4.

2. NUMERICAL SIMULATIONS

For our simulations, we use the hierarchical N-body code *pkdgrav*, which is suitable for this project because of its capability of managing collisions among hard spherical particles and to model at the same time the gravitational interactions between them (Richardson et al. 2005). Our rubble piles are thus represented by an ensemble of equal-size "smooth" spheres (no surface friction), held together as a group by mutual gravity alone and otherwise free to move relative to each other.

We started with a disperse cloud of these particles (with total $L = 0$) and allowed it to collapse under its own gravity. Adopting a restitution coefficient (ratio of rebound to impact speed) for collisions between spheres of 0.8 (the exact value adopted makes little difference in the final result, so long as there is some dissipation), kinetic energy is dissipated and the collapse results in a compact spherical aggregate, with all particles essentially in contact. The chaotic nature of this process produces a "natural" disordered packing (in contrast, ordered packing may introduce extra artificial resistance to reshaping; see Richardson et al. 2005; Walsh et al. 2008).

By carving out from this collapsed, disordered pile different ellipsoids composed of ∼1000 particles, we constructed 36 different triaxial rubble piles that sample the axial ratio plane (b/a, c/a) uniformly (Figure 4). A rigid rotation is then imposed on each body to obtain a given $\langle L\rangle$ value.

The above ellipsoids constitute the initial conditions of our simulations. Since they are far from fluid equilibrium, they quickly start to readjust their shape according to their angular momentum and density. As shown in Figure 4, not unexpectedly they are found to move toward a more stable (lower potential energy) state, asymptotically represented by fluid equilibrium. However, this state is never reached in practice, due to a small—but not negligible—compression-induced shear strength, and the evolution stops before the fluid equilibrium is attained. The global reshaping is rather fast (Figure 2), depending mainly on asteroid density (a few hours for asteroids of density $\sigma \sim 2000$ kg m^{-3}), and the simulations are allowed to continue long enough to ensure that the evolution is complete.

We analyzed the final states by measuring the shape and spin properties of the resulting configurations (as detailed in Richardson et al. 2005). Since we are interested in non-catastrophic evolutions, we discard cases exhibiting any mass losses (essentially for $\langle L\rangle > 0.5$). In turn, this choice allows us to assume that the observed shape changes occur at $\langle L\rangle \sim$ constant, thus simplifying the analysis.

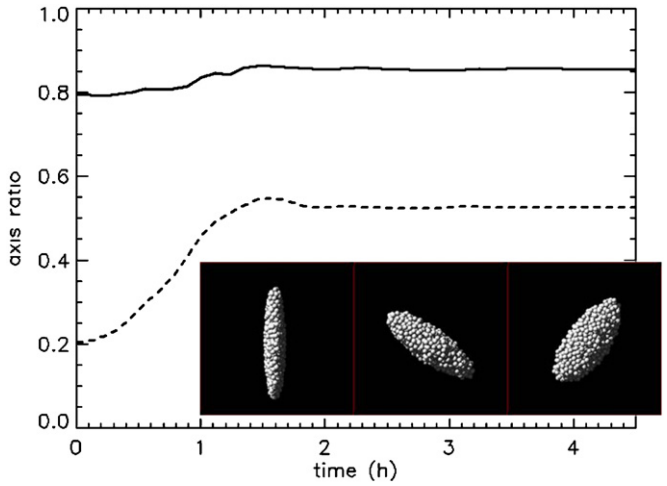

Figure 2. Time evolution of axis ratios (b/a: solid line; c/a: dashed line) in one of the simulations with $\langle L \rangle = 0.3$. The pictures of the body (polar views) correspond (left to right) to the initial conditions ($t = 0$), $t = 1$ hr, and $t = 2$ hr. The timescale of the evolution depends on the bulk density only (around 1250 kg m^{-3}, given the random packing of spheres of 2000 kg m^{-3}). The simulations are allowed to continue much longer to ensure that no further changes occur.

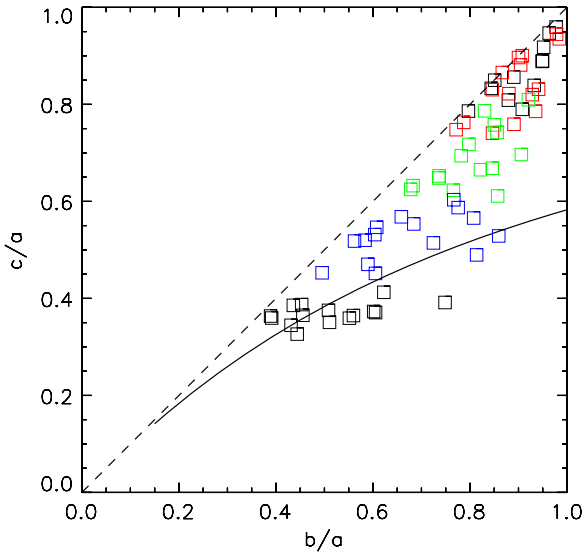

Figure 3. Set of final, stable points of our simulations, with $\langle L \rangle = (0.0, 0.1, 0.2, 0.3, 0.4)$. Each color corresponds to a different value of $\langle L \rangle$. Only objects undergoing uniform principal axis rotation are plotted, i.e., the cases with $b < c$ (which would lie above the diagonal) have been discarded, since they represent unstable situations. The solid line represents the Jacobi sequence. Note the similarity with the populated area shown in Figure 1. Inside this region, some differences exist that can be due both to the choice of our initial conditions and to observation bias. For example, slow-rotating bodies exhibiting light curves of low amplitude (i.e., $b/a,\ c/a > 0.8$) are probably underrepresented in the observed sample. The dashed line is the diagonal defining prolate ellipsoids with $b = c$.

The full set of end states from our simulations is shown in Figure 3. The striking similarity with the observed shape distribution (Figure 1) is immediately apparent.

Of course, we are aware that some of the real, observed asteroids might not in fact be rubble piles: it is conceivable that a fraction of them may be nearly monolithic bodies that never experienced catastrophic collisions (Bottke et al. 2005). The fraction of these "survivors" is not yet definitely established, and tends to be model dependent. Also, we note that a clear dependency of the distribution of Figure 1 on the object sizes seems to be absent. Conversely, we can say that our simulations give a good match to available observational data that, if true, generally supports the idea that even the largest asteroids could obey the general shape trend.

3. COMPARISON WITH THEORY AND INTERPRETATION

In order to understand how global reshaping can produce our results, we compared the evolution of the shape of each simulated body to gradients of the theoretical potential energy field for rotating ellipsoids. We computed several potential energy maps on the axial ratio plane, each one associated with a different normalized angular momentum (Figure 4). The result illustrates the extreme flatness of the potential energy field: the typical amplitude of variation (in the area populated by observed objects) is ∼10% at most. The theoretical Maclaurin and Jacobi minima for ideally fluid bodies are easily recognizable, and are surrounded by flat areas. A remarkable feature, particularly relevant for the following, is a valley of relative minimum that ends at the Maclaurin equilibrium. Originally represented by the diagonal of the shape plane for $\langle L \rangle = 0$, it bends and become narrower for larger $\langle L \rangle$, in such a way that the Maclaurin minimum is always at its lowest point (Figure 4). When the Jacobi solution appears ($\langle L \rangle > 0.3038$), it falls at the other end of the valley.

The evolution of our simulated rubble piles takes place at constant $\langle L \rangle$ (no mass loss) and exhibits the expected tendency to follow the gradient of the potential field (Figure 4), going toward lower values.

A general feature that can be observed (particularly evident for values of $\langle L \rangle \leqslant 0.2$) is the convergence of several evolution paths toward perfectly prolate shapes (having $a > b = c$), i.e., on the diagonal of the axis ratio plane or (for less elongated initial shapes) toward the valley whose bottom coincides with the Maclaurin minimum. For values of $\langle L \rangle$ immediately below the appearance of the Jacobi minimum ($\langle L \rangle \sim 0.3$), a corresponding flat region of the potential (around coordinates $[b/a,\ c/a] = [0.55, 0.45]$) appears and also attracts a subset of the bodies.

As expected, our simulated rubble piles do not behave like perfect fluids, due to their granular nature and ability to sustain shear stress, thus determining an end state that does not coincide, in general, with the fluid equilibrium points. However, a tendency to populate regions in the vicinity of the equilibrium point and, more generally, the valley, is evident.

We also estimated the friction angle associated with the spread of end states in Figure 4. In fact, each ellipsoidal state corresponds to a different slope of the surface relative to the local gravity. By assuming internal homogeneity, we computed the maximum angle, on the ellipsoid surface, between the local resultant of gravity and centrifugal force, and the normal to the local tangential plane. We find that the simulated asteroids that stop farther from the equilibrium points exhibit a typical maximum slope angle around 10° (Figure 4). This property is essentially due to the nature of our simulated bodies, composed of an unordered distribution of spheres without surface friction that are free to move around one another, and that are affected by only a small degree of interlocking. The situation is thus rather different from Richardson et al. (2005), in which the optimized hexagonal packing used to build initial conditions introduces an anisotropic response to stresses and results in a higher friction angle.

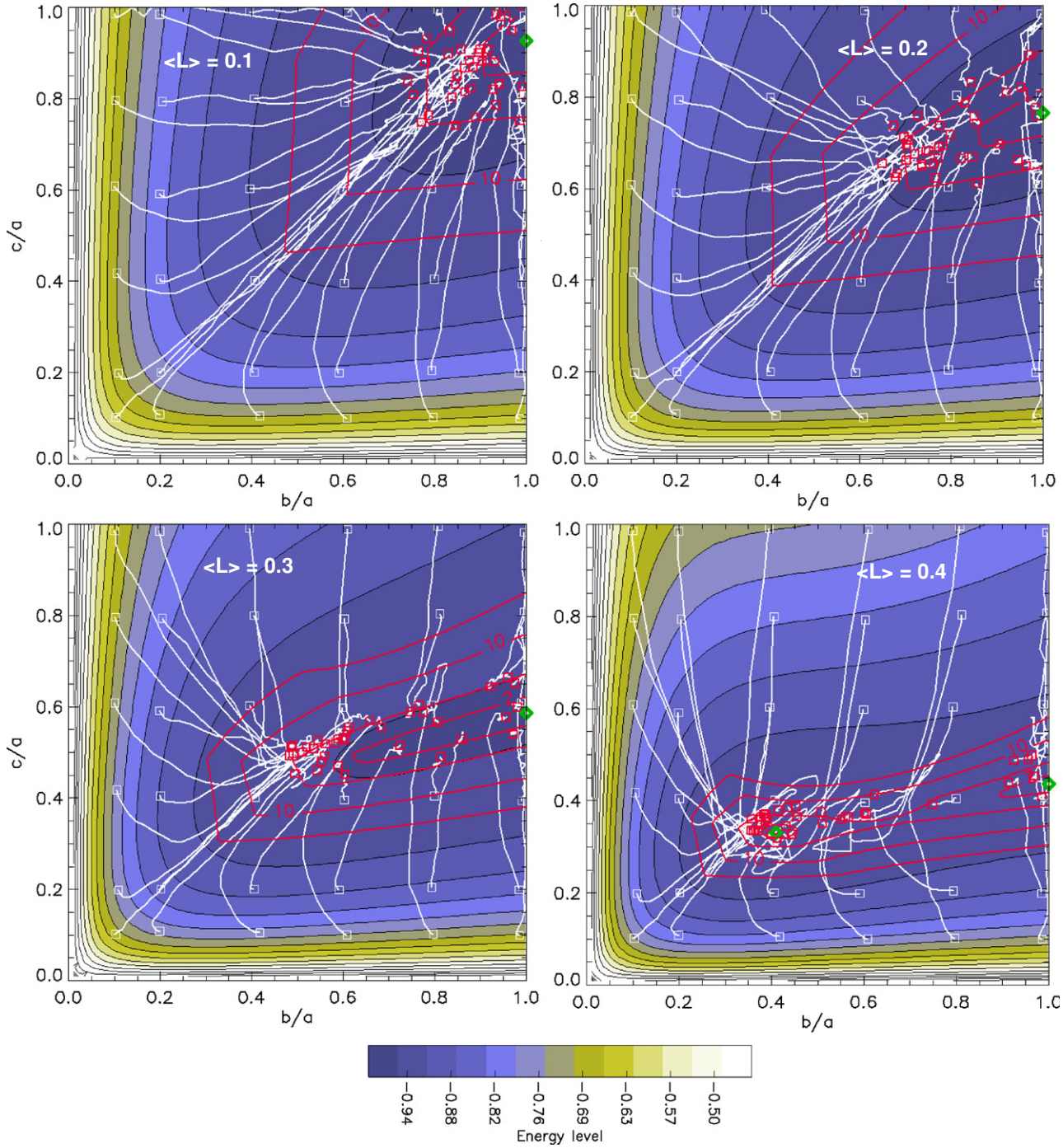

Figure 4. Evolution of asteroid shapes following the energy gradient on the $(b/a, c/a)$ plane, for four different values of the normalized angular momentum of a body $\langle L \rangle$. The color levels and the black isolines indicate the value of the total potential energy of a rotating ellipsoid (normalized to the absolute value of energy of a non-rotating sphere of the same density), computed as the sum of rotational energy and gravity potential. With the exception of extreme elongations (b/a or $c/a < 0.2$), the potential is very flat. The green diamonds represent the location of the fluid equilibrium points at the minima of the potential. For the two top panels and the bottom left panel, only the Maclaurin sequence exists, on the $b/a = 1$ axis. In the bottom right panel, the Jacobi minimum is also visible. The white lines represent the evolution paths of different ellipsoids in our simulations, approximately following the energy gradient. Their ending points are marked by a red square. The red isolines represent the maximum slope found on the surface of an ellipsoid having the corresponding axis ratios (for a given $\langle L \rangle$). Only the isolines for 2°, 5°, 10°, and 15°, numerically computed, are plotted. The maximum slope angle for our simulated bodies can be estimated by comparing the distribution of red dots to these isolines.

We checked this interpretation by means of two very different approaches. First, we computed particle–particle distance distributions during the evolution, looking for distance peaks corresponding to a crystalline structure. Then, we ran several simulations using some final states illustrated above as initial conditions, after having changed their spin rate. This forced, extended evolution could have shown a different behavior if internal crystallization had occurred. In both cases, no hints of crystallization were found.[9]

[9] We cannot exclude that in other conditions this could happen, such as, for example, after repeating the procedure several times. In a different context, this is the case of the simulations in Walsh et al. (2008), in which a forced spin change is continuously induced and a slow crystallization takes place on much longer timescales.

We stress here a fundamental result: when reaching the potential "valley," the objects are very close in potential energy to both the Maclaurin and the Jacobi sequence (<5% relative difference). They can thus be stable and close to fluid equilibrium, despite being fairly different in shape. As an example, a rather elongated prolate ellipsoid at $\langle L \rangle = 0.3$, having $b/a = 0.6$ and $c/a = 0.45$, is very close, in terms of energy, to the spheroid ($c/a = 0.58$ and $b = a$) at the same $\langle L \rangle$, but at fluid equilibrium on the Maclaurin sequence.

Nevertheless, the variety of final shapes obtained in our simulations appears to be strictly correlated with the location and extension of the potential valley, which changes depending on the total angular momentum of the system (Figure 3).

4. DISCUSSION

We have shown by numerical simulations and theoretical arguments that a reshaping process governed by the topology of the energy potential of rotating ellipsoids is compatible with the observed distribution of real asteroid shapes. We stress, however, that the low friction angle observed in our simulations is not necessarily characteristic of the asteroid constituent material. In fact, mechanisms capable of temporarily "fluidizing" granular aggregates exist, as discussed above. Incidentally, this also occurs during shear reversal observed in laboratory experiments (Utter & Behringer 2004). Our results suggest that, on asteroids, the action of random impacts, seismic shaking, or tides could produce similar effects, at least on the largest scales of an object. Our simulations, while not directly including these reshaping mechanisms, are in fact mimicking their fluidizing effect by using a low friction angle. This suggests that external mechanisms could enhance the mobility of the constituent blocks in a random way, without introducing systematic effects in the trend of shape change.

We can also try and relate our results to previous studies using the rotational properties. In fact, our plots show that a dependency between flattening and $\langle L \rangle$ (c/a decreasing for increasing $\langle L \rangle$, as in Chandrasekhar 1969) is preserved even for bodies that do not lie on the fluid equilibrium sequences. This provides us an opportunity to verify our results, by using the observed physical properties of large asteroids (diameters >100 km) that possess one or more small satellites (diameter ratio satellite/primary < 0.2). For these, the density uncertainty is lower than usual since the mass can be derived from applying Kepler's third law to the satellite orbits. They thus provide much better constraints than other objects (Hestroffer & Tanga 2005). These Main Belt binaries still have an uncertain origin, since they are generally too large for formation by YORP spin-up (Walsh et al. 2008). Most may have formed during post-catastrophic-disruption reaccumulation (Durda et al. 2004), so they should naturally be rubble piles.

Therefore we selected the seven best-characterized high-size-ratio binaries (Descamps & Marchis 2008), for which an ellipsoidal fit to the shape of the primary is available. We find (Figure 1) that they actually fall either not far from the diagonal of perfect prolate bodies ($b = c$), or on the Jacobi sequence.

It is very interesting to see that the relation between angular momentum $\langle L \rangle$ and flattening c/a is respected for binaries (Figure 5), supporting the idea that these asteroids underwent a reshaping process—each at its own, constant angular momentum—until they reached the stability valley, whose position in terms of flattening value is a function of $\langle L \rangle$ itself. If our model is correct, future observations of binaries should confirm this trend, provided that accurate mass and size determinations are obtained.

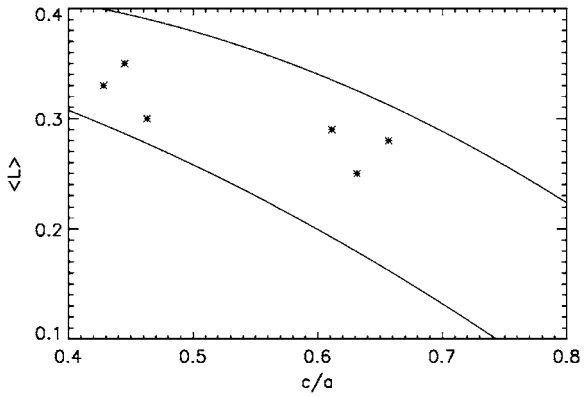

Figure 5. Normalized angular momentum $\langle L \rangle$ and flattening (c/a) of asteroids with one or more satellites. The region between the two lines represents the approximate range of stable end states in our simulations. For this plot, only high-size-ratio binaries with a small satellite (<20% of the primary size) whose ellipsoidal shape is known (from Kryszczynska et al. 2007) have been included (from left to right: 107 Camilla, 130 Elektra, 243 Ida, 45 Eugenia, 22 Kalliope, 87 Sylvia). The values refer to the primaries only, which dominate these systems in terms of angular momentum content. The general decreasing trend of $\langle L \rangle$ is consistent with our evolution scenario. The values of mass and size needed for this plot are taken from Descamps & Marchis (2008).

The results presented here are compatible with previous numerical studies simulating rubble piles by random packing (Tanga et al. 2009), and can be improved in several ways in future.

For example, polydisperse sphere sizes could be used to test the absence of any crystallization tendency (preliminary tests seem to indicate that the behavior is similar to the one illustrated here). Also, the energy potential analysis could be completed by a study of the force network among particles.

Eventually, the arbitrary distribution of our initial conditions could be substituted by the more realistic outcome of simulations of gravitational reaccumulation processes.

Despite these limitations, we believe that we have captured the fundamental properties of a general shape evolution process, in qualitative agreement with analytical models of granular materials in the continuum limit (although uncertainty remains on how to reconcile N-body macroscopic phenomena with the zero-grain-size limit; Holsapple 2009).

Future analysis of the physical properties of a larger number of asteroids, such as those to be obtained, for example, by the next generation of sky surveys like Gaia and Pan-STARRS, will help to better define the mechanisms that have sculpted the present shape distribution of the asteroids, and establish its consistency with an internal rubble-pile structure.

We thank P. Michel for the stimulating discussions. P.T. and C.C. acknowledge the support of the French Programme National de Planétologie (PNP). D.C.R. had support by the National Aeronautics and Space Administration under grant no. NNX08AM39G issued through the Office of Space Science and by the National Science Foundation under grant no. AST0708110. P.P. and A.C. have been supported by Italian Space Agency (ASI) funds. We thank the anonymous referee for help in improving this Letter.

Facilities: Mésocentre de Calcul-SIGAMM hosted at the Observatoire de la Côte d'Azur, Nice, France

REFERENCES

Bottke, W. F., et al. 2005, Icarus, 175, 111
Chandrasekhar, S. 1969, Ellipsoidal Figures of Equilibrium. The Silliman Foundation Lectures (New Haven, CT: Yale Univ. Press)
Davis, D. R., Durda, D. D., Marzari, F., Campo Bagatin, A., & Gil-Hutton, R. 2002, in Asteroids III, ed. W. F. Bottke, A. Cellino, P. Paolicchi, & R. P. Binzel (Tucson, AZ: Univ. Arizona Press), 545
Descamps, P., & Marchis, F. 2008, Icarus, 193, 74
Durda, D. D., et al. 2004, Icarus, 167, 382
Farinella, P., Paolicchi, P., Tedesco, E. F., & Zappalà, V. 1981, Icarus, 46, 114
Harris, A. W., Fahnestock, E. G., & Pravec, P. 2009, Icarus, 199, 310
Hestroffer, D., & Tanga, P. 2005, BAAS, 37, 1562
Hilton, J. L. 2002, in Asteroids III, ed. W. F. Bottke, A. Cellino, P. Paolicchi, & R. P. Binzel (Tucson, AZ: Univ. Arizona Press), 103
Holsapple, K. A. 2001, Icarus, 154, 432
Holsapple, K. A. 2004, Icarus, 172, 272
Holsapple, K. A. 2009, in Lunar and Planetary Institute Science Conference, (Technical Report, 40), 2053
Kaasalainen, M. 2004, A&A, 422, L39
Kaasalainen, M., Mottola, S., & Fulchignoni, M. 2002, in Asteroids III, ed. W. F. Bottke et al. (Tucson, AZ: Univ. Arizona Press), 139
Korycansky, D. G., & Asphaug, E. 2003, Icarus, 163, 374
Kitazato, K., Abe, M., Ishiguro, M., & Ip, W. H. 2007, A&A, 472, L5
Kryszczynska, A., La Spina, A., Paolicchi, P., Harris, A. W., Breiter, S., & Pravec, P. 2007, Icarus, 192, 223 (http://vesta.astro.amu.edu.pl/Science/Asteroids/)
Michel, P., Benz, W., Tanga, P., & Richardson, D. C. 2001, Science, 294, 1696
Richardson, D. C., Elankumaran, P., & Sanderson, R. E. 2005, Icarus, 173, 349
Sánchez, P., & Scheeres, D. J. 2009, in 40th Lunar and Planetary Science Conference, (Technical Report, 40), 2228
Sharma, I., Jenkins, J. T., & Burns, J. A. 2009, Icarus, 200, 304
Tanga, P., Hestroffer, D., Delbo, M., & Richardson, D. C. 2009, Planet. Space Sci., 57, 193
Torppa, J., Hentunen, V.-P., Pääkkönen, P., Kehusmaa, P., & Muinonen, K. 2008, Icarus, 198, 91
Utter, B., & Behringer, R. P. 2004, Eur. Phys. J. E, 14, 373
Vokrouhlicky, D., Breiter, S., Nesvorny, D., & Bottke, W. F. 2007, Icarus, 191, 636
Walsh, K. J., Richardson, D. C., & Michel, P. 2008, Nature, 454, 188